On steering a sailing ship in a wearing maneuver

Jouffroy, Jerome

Publication date:
2009

Document version
Final published version

Citation for pulished version (APA):
Jouffroy, J. (2009). *On steering a sailing ship in a wearing maneuver*. Paper presented at IFAC International Conference on Manoeuvering and Control of Marine Craft, .

Preprints of the 8th IFAC International Conference on Manoeuvring and Control of Marine Craft, September 16-18, 2009
Casa Grande Hotel, Guarujá (SP), Brazil

On Steering a Sailing Ship in a Wearing Maneuver

Jerome Jouffroy *

* *Mads Clausen Institute*
University of Southern Denmark (SDU)
Alsion 2, DK-6400 Sønderborg, Denmark
e-mail: jerome@mci.sdu.dk

Abstract: Compared to more conventional ships, little attention was given to nonlinear control design for ships sailing by the wind. Following our previous work, this paper addresses the issue of trajectory and reference input generation for a model that imitates the general behavior of sailing vessels. Specifically, we consider the generation of paths to perform a wearing maneuver. A feedforward controller scheme is then introduced to steer the modeled vehicle along this maneuver, and simulation results are presented as an illustration.

Keywords: Sailing ships, path generation, steering control, nonlinear systems.

1. INTRODUCTION

Automatic control systems are now ubiquitous aboard fuel-propelled ships, and the research community in this area has been active for many years now, producing a wealth of results, both of theoretical and practical importance. In comparison, much less attention was given to designing control strategies for ships whose means of propulsion is the wind, and only a few papers deal with sailing ships. Most of these studies, such as Yeh and Bin (1992) and Aartrijk et al. (1999), consider Artificial Intelligence-based techniques for the control strategies and do not make use of the available dynamic models that would allow for further analysis to assess for example stability or performance. Other references, Xiao and Austin (2000), or Elkaim and Boyce (2006), adopt a more traditional model-based perspective, but their control design is mostly based on a linear model structure, thus not allowing for the study of dynamical aspects and maneuvers that are specific to sailing vehicles, such as tacking, jibing or wearing.

In sailing, one of the main concerns is to generate a feasible path that would take into account these specificities. Of interest is also to compute the corresponding reference input signals that will result in the vehicle following the chosen path/trajectory, thus paving the way for feedback control strategies to track the desired trajectories. In marine control, this is the task of guidance systems, that typically use simplified models to compute feasible trajectories (see (Fossen, 2002, chapter 5)).

Following our previous work (see Jouffroy (2009)), this paper is a preliminary study towards trajectory and reference input generation that would take into account the global dynamic of sailing vessels. More specifically, we consider hereafter the particular case of what is known as a wearing maneuver for square-rigged vessels (see Harland (1984)), i.e. when a ship performs jibes to go upwind. After this introduction, we introduce a very simple model allowing to dynamically mimic the constraints represented by the no-go zone in sailing. Then, the following section gives a method to generate paths for a wearing maneuver that are continuous in curvature. Section 4 introduces a control strategy to compute input signals allowing our model to perfom the maneuver, and some simulation results are briefly presented. Finally, a few concluding remarks end the paper.

2. A PHENOMENOLOGICAL MODEL

Instead of making a full model of a particular sailing ship based on first principles (see for example Fossen (2002) for conventional ships), we would like to have at our disposal a model that would be simple enough for our trajectory and path generation purposes, while still retaining the basic dynamic behavior necessary to construct feasible paths that are particular to sailing vessels. An example of this is the well-known zig-zag pattern that a sailboat follows when perfoming a tacking maneuver to go upwind.

Indeed, one of the main difference of sailing systems with more conventional vehicles such as ships or cars, is that their propulsion is dependent on the external environment. More precisely, this is dependent on the orientation of the propulsive system (a sail, but also a kite) in the air flow, and because of this there are some orientations of the vehicle that provide no propulsion, the so-called no-go zone (see figure 1).

Following our previous work (see Jouffroy (2009)), consider hence the following set of differential equations

$$\dot{x}(t) = u(t)\cos\psi(t) \tag{1}$$
$$\dot{y}(t) = u(t)\sin\psi(t) \tag{2}$$
$$\dot{\psi}(t) = u(t)s(\delta(t)) \tag{3}$$
$$m\dot{u}(t) + du(t) = d.\rho(\psi(t), u_s(t)), \tag{4}$$

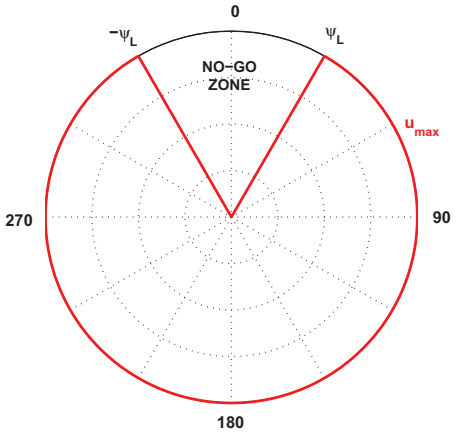

Fig. 1. Polar curve of the propulsive system

where x, y are the earth-fixed positions, ψ the heading angle, u the surge velocity, and δ the rudder angle (see figure 2). We assume δ is limited to be within the interval $[-\delta_L, \delta_L]$, where $0 < \delta_L < \pi/2$. The term $s(\bullet)$ is a stricly monotonic and odd function defined on $[-\delta_L, \delta_L]$. Because of this property, and of the constraints on δ, $\delta(t)$ can be readily deduced from s and in the following we will simple write $s(t)$ instead of $s(\delta(t))$. The parameter m combines both the mass of the boat together with its added mass, while d is a linear damping term in surge.

The term $\rho(\psi(t), u_s(t))$ is the positive nonlinear function

$$\rho(\psi(t), u_s(t)) = \begin{cases} 0 & if\ |\psi(t)| \leq \psi_L \\ sat_{u_{\max}}(u_s(t)) & otherwise \end{cases} \quad (5)$$

which plays a role similar to performance polar diagrams well-known in sailing (Marchaj (1990), Richards et al. (2001)) (see figure 1). The constant angle ψ_L indicates the limits of the no-go zone, while $u_s(t)$ is a control input signal, saturating at $u_{\max}$, that can be seen as the attainable surge velocity as provided by the tuning of the propulsive system.

Note that in equations (1)-(4), we have assumed that the wind is coming from the North. This can easily be generalized to any direction by a simple change of coordinates. Also, we assume the absence of any sea current. Additionally, since we want to focus, in our control scheme, on the effect of the orientation of the propulsive system in the wind, and that the main direction of motion is longitudinal, we consider only simplified dynamics in surge, the other modes being neglected. Note that similar simplifications are considered in some sailboat models (see for example Davies (1990)).

Function (5) can also be easily generalized to consider more realistic polar diagrams corresponding to particular boats. However, the simple form of (5) already allows us to describe a pattern quite common to many sailing vehicles through the dead zone between $-\psi_L$ and ψ_L (see figure 1). Indeed, a trait common to all boats is that when operating a tacking maneuver, the ship will cross this dead zone, or no-go zone. And it is, roughly speaking, the inertia of the ship that will help it to do so, and to re-capture energy

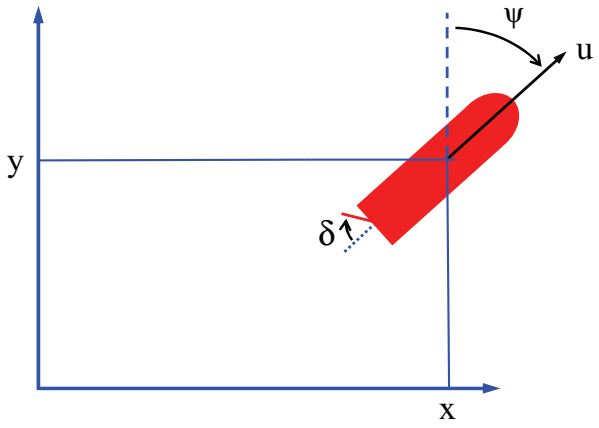

Fig. 2. Variable definition of our sailing vehicle

once on the other side. A corollary of this behavior is that if the vehicle speed before entering the dead zone is not high enough, its energy will not be sufficient to cross it entirely, and the ship will be said to be "in irons".

To see this, assume we start with a heading on the limit of the no-go zone, *i.e.* $\psi(0) = -\psi_L$. We want to cross the dead zone, hence we would like the heading to reach an angle $\psi(t) > \psi_L$ at some instant t. First, note that while in the dead zone, the wind does not propel the vehicle. Hence (4) and (5) imply simply that

$$m\dot{u}(t) + du(t) = 0, u(0) = u_0. \quad (6)$$

Solving this linear differential equation gives

$$u(t) = u_0 e^{-\frac{d}{m}t}. \quad (7)$$

Hence, in the dead zone, the dynamics for the heading are

$$\dot{\psi}(t) = u_0 e^{-\frac{d}{m}t} s(t), \psi(0) = -\psi_L. \quad (8)$$

Integrating (8), we get

$$\psi(t) = u_0 \int_0^t e^{-\frac{d}{m}\tau} s(\tau) d\tau - \psi_L. \quad (9)$$

Because of the properties of the function $s(\bullet)$, since $\delta(t)$ is bounded, so is $s(\bullet)$, and we will denote $\bar{s}$ the bound such that $|s(t)| \leq \bar{s}$. This, together with (8), implies the following inequality

$$\psi(t) \leq u_0 \int_0^t e^{-\frac{d}{m}\tau} \bar{s} d\tau - \psi_L \quad (10)$$

which, after integration, leads to

$$\begin{aligned} \psi(t) &\leq u \frac{m}{d}_0 \bar{s} \left(1 - e^{-\frac{d}{m}t}\right) - \psi_L \\ &\leq u_0 \frac{m}{d} \bar{s} - \psi_L \end{aligned} \quad (11)$$

From (11), it is clear that with fixed parameters $\bar{s}$, m, d and ψ_L, the vehicle will never cross the dead zone entirely, or reach $\psi(t) > \psi_L$ if u_0 is too small, *i.e.* if

$$u_0 \frac{m}{d} \bar{s} - \psi_L < \psi_L, \quad (12)$$

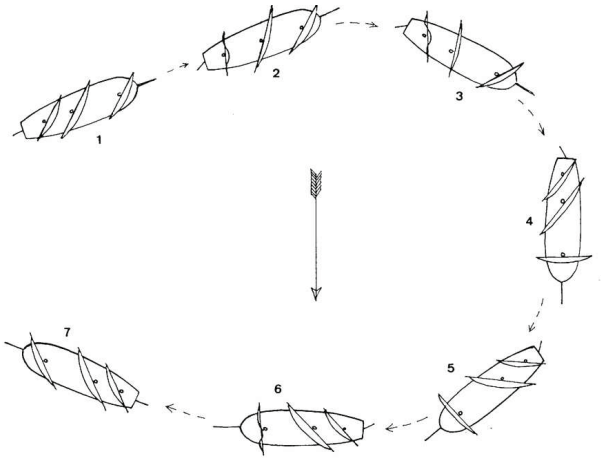

Fig. 3. Wearing maneuver for a three-mast square-rigger

which gives the following inequality constraint on u_0:

$$u_0 < 2\psi_L \frac{\psi_L}{\bar{s}} \frac{d}{m}. \tag{13}$$

3. CREATING WEARING PATHS

Assume that we are given a set of way-points where each segment connecting a pair of way-points is compatible with the navigation specifics of a sailing vessel, *i.e.* its heading is outside the no-go zone. In the following, we focus on describing and generating a path for a loop that would connect two adjacent segments, and thus perfom a wearing maneuver (see figure 3).

Hence, consider we are given three way-points p_1, p_2, p_3 as pictured in figure 4. In the following, we define each way-point p_i by the triple (x_i, y_i, ψ_i), also known as "posture" in robotics (see Kanayama and Hartman (1989)). Without loss of generality and for the sake of simplicity, we assume that $y_1 = y_2 = 0$, as in figure 4. Also, ψ_i will always be tangent to the first segment it belongs to.

Obviously, the path generated by segments $[p_1, p_2]$ and $[p_2, p_3]$ has a singularity at p_2, and it is therefore not feasible for a sailing vessel. Using a conventional method, one would typically alternate straight lines and circles to construct a path, and that of a wearing maneuver could be constructed by doing so.

Instead, we will make use of a combination of clothoids and straight lines as pictured in figure 4. Frequently used in robotics (see for example Kanayama and Hartman (1989)), but also railways and road contruction, paths generated using clothoids have the advantage of having a continuous curvature, thus avoiding the above-mentionned discontinuity issue (discontinuity that is also present when using the lines/circles combination). Hence, following loosely the method introduced in Fleury et al. (1995), we describe briefly below how to generate a smooth wearing path.

First, replace p_2 with three new way-points $p_{2,1}$, $p_{2,2}$, $p_{2,3}$ (see figure 4), thus creating the new segments or subpaths $[p_1, p_{2,1}]$, $[p_{2,1}, p_{2,2}]$, $[p_{2,2}, p_{2,3}]$ and $[p_{2,3}, p_3]$, the two middle ones being clothoid arcs, while the two remaining ones are straight lines. Let α be the angle between the two original segments $[p_1, p_2]$ and $[p_2, p_3]$. Way-point $p_{2,2}$ is set at a distance b from p_2 and defined as

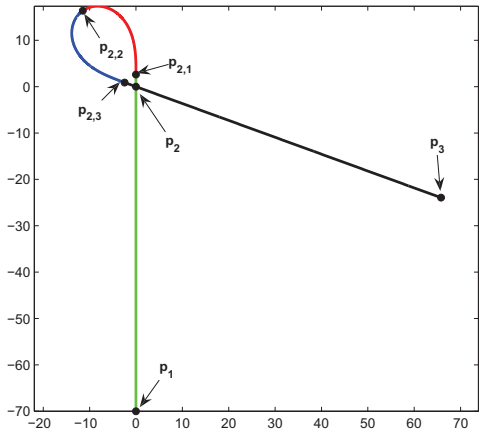

Fig. 4. A wearing maneuver using clothoids.

$$p_{2,2} = \begin{bmatrix} b\cos\left(-\frac{\alpha}{2}\right) + x_2 \\ b\sin\left(-\frac{\alpha}{2}\right) \\ -\frac{\pi+\alpha}{2} \end{bmatrix}. \tag{14}$$

This posture is linked by a clothoid arc to

$$p_{2,1} = \begin{bmatrix} x_{2,1} \\ 0 \\ 0 \end{bmatrix}, \tag{15}$$

where $x_{2,1}$ is to be defined later.

A clothoid is a curve whose tangent vector is a quadratic function of the path parameter σ, and that can be written as follows.

$$\psi(\sigma) = \frac{k}{2}\sigma^2 + \kappa_0\sigma + \psi(0) \tag{16}$$

where k is a shape parameter, κ_0 the initial curvature, and $\psi(0)$ the initial heading. Using (16), the path followed by a clothoid arc can then be written as follows.

$$x(\sigma) = A\int_0^\sigma \cos\psi(\tau)d\tau + x(0) \tag{17}$$

and

$$y(\sigma) = A\int_0^\sigma \sin\psi(\tau)d\tau + y(0) \tag{18}$$

where σ is a path variable evolving between 0 and 1, A is a constant positive scaling factor, and $x(0)$ and $y(0)$ are the initial positions of the arc.

We would like now to get the values of k, κ_0, $\psi(0)$, $x(0)$, $y(0)$ and A to link $p_{2,1}$ and $p_{2,2}$. To do so, first assume that for this segment, $p_{2,1} = (x(0), y(0), \psi(0))$ and $p_{2,2} = (x(1), y(1), \psi(1))$. This first leads, in (16), to $\psi(0) = 0$. Then, since $p_{2,1}$ is also connected to a straight line, the curvature at this point is zero, and $\kappa_0 = 0$. Finally, since from (14) we have that $\psi(1) = -\frac{\pi+\alpha}{2} = \psi_{2,2}$, resulting in

$$k = 2\psi_{2,2}, \tag{19}$$

which in turn gives, at $\sigma = 1$,

$$x_{2,2} = x(1) = A \int_0^1 \cos(\psi_{2,2}\tau^2)d\tau + x(0) \tag{20}$$

and

$$y_{2,2} = y(1) = A \int_0^1 \sin(\psi_{2,2}\tau^2)d\tau + y(0), \tag{21}$$

where $y(0) = 0$ since the clothoid should be the direct prolongation of straight segment $[p_1, p_{2,1}]$. However, if $p_{2,2}$ was precisely on p_2, $x_{2,2}$ would be known and equations (20) and (21) would be an overdetermined system with the only unknown parameter A. Consequently, $x(0) = x_{2,1}$ must also be determined through (20) and (21). Thus we have

$$A = y_{2,2} / \int_0^1 \sin(\psi_{2,2}\tau^2)d\tau \tag{22}$$

and

$$x(0) = x_{2,1} = x_{2,2} - A \int_0^1 \cos(\psi_{2,2}\tau^2)d\tau. \tag{23}$$

Subpath $[p_1, p_{2,1}]$ is then straightforward to obtain. Indeed, assuming this time that p_1 corresponds to $\sigma = 0$, while $p_{2,1}$ corresponds to $\sigma = 1$, knowing that $\psi(\sigma)$ is always set to 0 gives ($y(\sigma) = 0$)

$$x(\sigma) = A \int_0^\sigma d\tau + x(0), \tag{24}$$

and since $x(0) = x_1$ and $x(1) = x_{2,1}$, we simply have

$$A = x_{2,1} - x_1 \tag{25}$$

for this particular segment.

Finally, paths for segments $[p_{2,2}, p_{2,3}]$ and $[p_{2,3}, p_3]$ are readily obtained by symmetry with respect to the line going through (x_2, y_2) and $(x_{2,2}, y_{2,2})$ (see figure 4).

4. FOLLOWING THE PATH

Once the paths corresponding to a wearing maneuver are defined, our objective is to find appropriate control signals that will steer the vehicle along these paths. Since we are in a "wearing maneuver" configuration, the vehicle will not be moving in and out of the no-go zone like in a tacking maneuver (see Jouffroy (2009)). Because of this, the input $u_s(t)$ will mostly affect the speed of the vehicle on the path. Hence it will in the following be assumed that $u_s(t) = u_{\max}$, *i.e.* the maximum speed that can be made out of the wind.

However, the value of the steering function $s(t)$ at a particular instant will be influenced by the vehicle position on the path, hence on $u(t)$ generated by $u_s(t)$. To see this, rewrite (1)-(3) to obtain dynamics in $\sigma(t)$ as follows.

$$\frac{dx}{d\sigma}(\sigma(t))\dot{\sigma}(t) = u(t)\cos\psi(t) \tag{26}$$

$$\frac{dy}{d\sigma}(\sigma(t))\dot{\sigma}(t) = u(t)\sin\psi(t) \tag{27}$$

$$\frac{d\psi}{d\sigma}(\sigma(t))\dot{\sigma}(t) = u(t)s(t) \tag{28}$$

Isolating $s(t)$ in (28), we obtain

$$s(t) = \frac{1}{u(t)}\frac{d\psi}{d\sigma}(\sigma(t))\dot{\sigma}(t). \tag{29}$$

Then, squaring (26) and (27) gives

$$\left[\left(\frac{dx}{d\sigma}(\sigma(t))\right)^2 + \left(\frac{dy}{d\sigma}(\sigma(t))\right)^2\right]\dot{\sigma}^2(t) = u^2(t) \tag{30}$$

which, knowing that both $u(t)$ and $\dot{\sigma}(t)$ are always positive, gives the following first-order differential equation

$$\dot{\sigma}(t) = u(t)\frac{1}{\sqrt{\left(\frac{dx}{d\sigma}(\sigma(t))\right)^2 + \left(\frac{dy}{d\sigma}(\sigma(t))\right)^2}}, \tag{31}$$

where we assume that parameter $\sigma(t)$ takes zero value on the beginning of the path, i.e. $\sigma(0) = 0$. Then, using (31) in (29), we get

$$s(t) = \frac{d\psi}{d\sigma}(\sigma(t))\left[\left(\frac{dx}{d\sigma}(\sigma(t))\right)^2 + \left(\frac{dy}{d\sigma}(\sigma(t))\right)^2\right]^{-\frac{1}{2}}. \tag{32}$$

Hence, (31) and (32) can be seen as a state-space realization of an inverse system (see (Sastry, 1999, chapter 9)), whose output is the steering function $s(t)$ and whose input is the velocity of the vehicle $u(t)$.

The dynamics of the state-equation (31) is driven by the evolution of the term $\left(\frac{dx}{d\sigma}(\sigma(t))\right)^2 + \left(\frac{dy}{d\sigma}(\sigma(t))\right)^2$. It can be verified that, whether a straight line or a clothoid, this term equals to the value of $A^2(\sigma)$ on the same segment (*i.e.* similar to (22) on a clothoid arc, or to (25) on a straight line). Indeed, on a straight path, we have

$$\frac{dx}{d\sigma}(\sigma) = A(\sigma)\cos\psi_C \tag{33}$$

and

$$\frac{dy}{d\sigma}(\sigma) = A(\sigma)\sin\psi_C, \tag{34}$$

with ψ_C a constant, whereas on a clothoid segment,

$$\frac{dx}{d\sigma}(\sigma) = A(\sigma)\cos\psi(\sigma) \tag{35}$$

and

$$\frac{dy}{d\sigma}(\sigma) = A(\sigma)\sin\psi(\sigma). \tag{36}$$

With this in mind, replace (31) with

$$\dot{\sigma}(t) = \frac{u(t)}{A(\sigma(t))} \tag{37}$$

and (32) with

$$s(t) = \frac{1}{A(\sigma(t))}\frac{d\psi}{d\sigma}(\sigma(t)). \tag{38}$$

Similarly, the term $\frac{d\psi}{d\sigma}(\sigma)$ can be computed for each segment of the path. For a straight line starting at $\sigma = 0$ and finishing at $\sigma = 1$, we have $\psi(\sigma) = \psi_C$, which leads to

$$\frac{d\psi}{d\sigma}(\sigma) = 0, \tag{39}$$

whereas for a clothoid arc on the same interval and linking a straight line to another clothoid arc, we have

$$\frac{d\psi}{d\sigma}(\sigma) = k\sigma. \tag{40}$$

Thus, equation (37) and (38) will be seen as a multi-model dynamical system, where the model, parametrized by $A(\sigma)$, will be switched according to which segment of the path the vehicle is currently evolving on.

As yet another difference of some sailing vehicles with more conventional vehicles is the unavailability of braking action to stop at the desired position. Mathematically, this action typically translates into a negative control input, on the thrusters of a conventional ship for example.

Because of the structure of the model in (4), and of the positive function (5), such an action is not possible. Hence we have to rely on the inertia of the system and release the sail at the right moment to stop at the desired location. In (4), this simply corresponds to letting $u_s(t) = 0$, i.e. switching off this control input at a definite instant t_{SO}.

Switching off $u_s(t)$ amounts to having dynamics (6), and a simple but useful remark can be made from this system. Indeed, because (6) is an autonomous stable linear differential equation, it is clear that reaching zero velocity will take an infinite amount of time (note henceforth that finite horizon techniques for motion planning (see for example Murray and Sastry (1993)) do not apply in this case).

Then, note that integrating $u(t)$ gives

$$\int_{t_2}^{t_1} u(\tau)d\tau = \int_{t_2}^{t_1} \sqrt{\dot{x}^2(\tau) + \dot{y}^2(\tau)}d\tau := l(t_2) - l(t_1) \tag{41}$$

where $l(t)$ is the arclength of the maneuver at time t ($l(0) = 0$). Thus, using (7) in (41), we get

$$l(t_2) = u(t_1) \int_{t_1}^{t_2} e^{-\frac{d}{m}(\tau - t_1)}d\tau + l(t_1) \tag{42}$$

which, after integration, gives

$$l(t_2) = u(t_1) \left(-\frac{m}{d} e^{-\frac{d}{m}(t_2 - t_1)} + \frac{m}{d} \right) + l(t_1) \tag{43}$$

Then letting $l_\infty := \lim_{t_2 \to \infty} l(t_2)$ and $t_{SO} := t_1$, we get

$$l_\infty = \frac{m}{d} u(t_{SO}) + l(t_{SO}) \tag{44}$$

Equation (44) means that if one wants to reach the point on the path with arclength l_∞, and then stay there, then the control input $u_s(t)$ should be switched off at the time t_{SO} when condition (44) is satisfied.

Note that another way to interpret this is to rewrite (44) as

$$u(t_{SO}) = \frac{d}{m} \left(l_\infty - l(t_{SO}) \right), \tag{45}$$

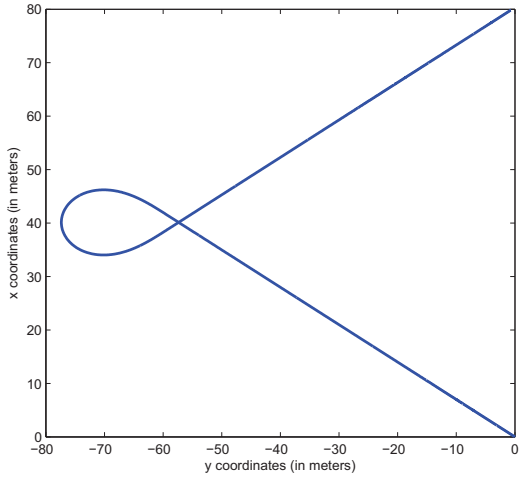

Fig. 5. Trajectory followed by the sailing vehicle.

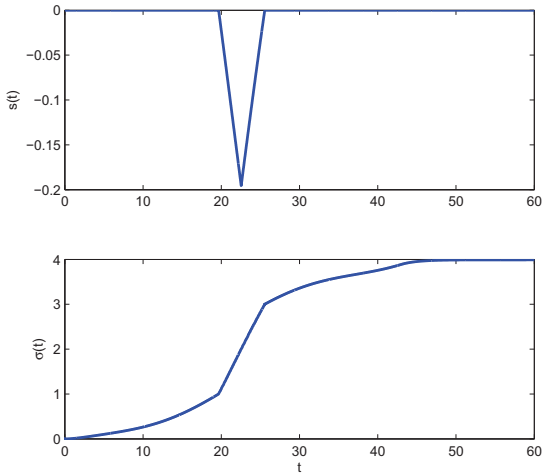

Fig. 6. Steering variable $s(t)$ and parameter $\sigma(t)$.

which expresses the fact that if the velocity of the vehicle is big enough, its energy will be sufficient to cover the distance $l_\infty - l(t_{SO})$. Before t_{SO}, we have

$$m\dot{u}(t) + du(t) = du_{\max} \tag{46}$$

and $u(t)$ is not yet enough to reach the desired point without propulsion.

To briefly illustrate the behavior of the dynamic controller (37) and (38), and of switch-off condition (44), hereafter are presented simulation results for a single wearing loop, with $m = 200$ and $d = 100$. Paths containing more wearing maneuvers can simply be composed of such loops. The trajectory of the vehicle in the xy-plane can be seen in figure 5, with initial position $x(0) = 0$ and $y(0) = 0$.

For implementation considerations, a continuous parametrization in σ was adopted, where each interval $\sigma \in [0, 1)$, $\sigma \in [1, 2)$, $\sigma \in [2, 3)$ and $\sigma \in [3, 4]$ corresponds to a different segment of the wearing path, and for which one will have different values $A(\sigma)$ and $\frac{d\psi}{d\sigma}(\sigma)$. Figure 6 shows the evolution of $\sigma(t)$ given by (37) as well as the corresponding steering function $s(t)$.

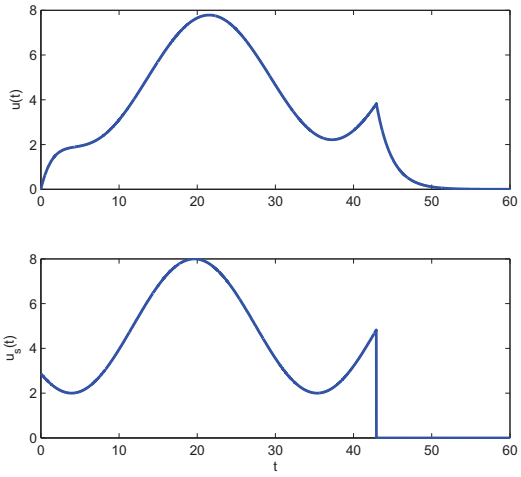

Fig. 7. Surge variable $u(t)$ and control input $u_s(t)$.

Note that the control strategy used in this paper also somewhat accounts for changes in wind speed, in the sense that related parameter $u_{\max}$ is allowed to vary in time. Figure 7 reflects this last point, where the evolution of $u_s(t)$ can be seen. Note also the effect of switch-off condition (44) (after $t = 40s$) on the surge velocity $u(t)$, that exponentially decreases to zero after t_{SO}.

5. CONCLUDING REMARKS

This paper reported on a study of nonlinear aspects for trajectory and reference input generation for sailing vessels. The models used seem to be simple enough to allow for motion planning purposes, but yet complex enough to reflect behaviors that are specific to sailing vehicles. Further work will include examining different important questions such as feedback control to maintain the vehicle on the path, and testing of the proposed strategies on models based on first principles.

REFERENCES

R. L. Van Aartrijk, C. P. Tagliola, and P. W. Adriaans. AI on the ocean: the robosail project. In *Proc. of the 15th European Conf. on Artificial Intelligence*, Lyon, France, 1999.

N. S. Davies. A real-time yacht simulator. Master's thesis, University of Auckland, 1990.

H. G. Elkaim and C. O. Boyce. Station keeping and segmented trajectory control of a wind-propelled autonomous catamaran. In *Proc. IEEE Conf. on Decision and Control*, San Diego, CA, 2006.

S. Fleury, P. Soueres, J.-P. Laumond, and R. Chatila. Primitives for smoothing mobile robot trajectories. *IEEE Transactions on Robotics and Automation*, 11(3): 441–448, 1995.

T. I. Fossen. *Marine Control Systems: Guidance, Navigation and Control of Ships, Rigs and Underwater vehicles.* Marine Cybernetics, 2002.

J. Harland. *Seamanship in the age of sail.* Naval Institute Press, 1984.

J. Jouffroy. A control strategy for steering an autonomous surface sailing vehicle in a tacking maneuver. In *Proc. IEEE Int. Conf. on Systems, Man, and Cybernetics*, San Antonio, Texas, 2009.

Y. Kanayama and B. I. Hartman. Smooth local path planning for autonomous vehicles. In *Proc. IEEE Int. Conf. on Robotics and Automation*, Scottsdale, AZ, 1989.

C. A. Marchaj. *Aero-hydrodynamics of sailing.* International Marine Publishing, 1990.

R. M. Murray and S. S. Sastry. Nonholonomic motion planning: steering using sinusoids. *IEEE Transactions on Automatic Control*, 38(5):700–716, 1993.

P. J. Richards, A. Johnson, and A. Stanton. America's cup downwind sails–vertical wings or horizontal parachutes? *Journal of Wind Engineering and Industrial Aerodynamics*, 89:1565–1577, 2001.

S. Sastry. *Nonlinear systems.* Springer, 1999.

C. M. Xiao and P. C. Austin. Yacht modelling and adaptive control. In *Proc. IFAC Conf. on Manoeuvering and Control of Marine Craft*, Aalborg, Denmark, 2000.

E. C. Yeh and J.-C. Bin. Fuzzy control for self-steering of a sailboat. In *Proc. of the Singapore Int. Conf. on Intelligent Control and Instrumentation*, 1992.